

CONFIDENTIAL

C-2
Copy 6
RM L54A08

NACA RM L54A08



RESEARCH MEMORANDUM

TRANSONIC WIND-TUNNEL INVESTIGATION OF THE
EFFECTS OF BODY INDENTATION FOR BOATTAIL AND CYLINDRICAL
AFTERBODY SHAPES ON THE AERODYNAMIC CHARACTERISTICS OF
AN UNSWEPT-WING—BODY COMBINATION

By Thomas C. Kelly

Langley Aeronautical Laboratory
Langley Field, Va.

CLASSIFICATION CHANGED

To UNCLASSIFIED

NACA Review also

effective
Oct. 14, 1957

Authority of *Y RN-121* Date CLASSIFIED DOCUMENT

Am 11-15-57

This material contains information affecting the National Defense of the United States within the meaning of the espionage laws, Title 18, U.S.C., Secs. 793 and 794, the transmission or revelation of which in any manner to an unauthorized person is prohibited by law.

NATIONAL ADVISORY COMMITTEE
FOR AERONAUTICS

WASHINGTON

March 15, 1954

LANGLEY AERONAUTICAL LABORATORY
LANGLEY FIELD, VIRGINIA

CONFIDENTIAL



NATIONAL ADVISORY COMMITTEE FOR AERONAUTICS

RESEARCH MEMORANDUM

TRANSONIC WIND-TUNNEL INVESTIGATION OF THE
EFFECTS OF BODY INDENTATION FOR BOATTAIL AND CYLINDRICAL
AFTERBODY SHAPES ON THE AERODYNAMIC CHARACTERISTICS OF
AN UNSWEPT-WING—BODY COMBINATION

By Thomas C. Kelly

SUMMARY

An investigation has been conducted in the Langley 8-foot transonic tunnel to study the effects of body indentation and afterbody shape on the aerodynamic characteristics of an unswept-wing—body combination.

Body indentation for a boattail configuration resulted in a considerable reduction in drag up to the highest lift coefficients tested ($C_L \approx 0.6$) at Mach numbers from 0.96 to 1.15. The transonic drag rise for a cylindrical afterbody configuration was less severe than that for a boattail configuration, while the use of body indentation with both configurations resulted in nearly the same proportional reductions of the transonic drag rise at a Mach number of 1.0. Maximum lift-drag ratios for the boattail configuration were increased at Mach numbers higher than 0.93 by indentation, the increase at a Mach number of 1.0 amounting to 16 percent.

INTRODUCTION

Several experimental investigations (refs. 1 to 3) have indicated that body indentation, as specified by the area rule (ref. 1), may result in an elimination or marked reduction of the transonic drag rise associated with the wing of a wing-body combination. Also, earlier investigations (ref. 4, for example) have shown that afterbody shape may have a significant effect on the drag rise associated with the wing.

The present investigation was conducted in the Langley 8-foot transonic tunnel to study the combined effects of body indentation and afterbody shape on the aerodynamic characteristics of a modified version

~~CONFIDENTIAL~~

of the unswept-wing-body combination reported in reference 2. The cylindrical afterbody of reference 2 was modified so that it was boat-tailed and the outer 20 percent of the wing span was removed in order to provide a configuration more typical of present-day design. In addition, two bodies of revolution, one having the same axial distribution of cross-sectional area as the present basic or unindented wing-body combination and the other having the same cross-sectional area distribution as the indented wing-body combination, have been tested to provide further experimental verification of the transonic drag-rise rule. Data have been obtained at Mach numbers from 0.80 to 1.15 and angles of attack from 0° to 8° .

SYMBOLS

M	average free-stream Mach number
q	free-stream dynamic pressure, lb/sq ft
\bar{c}	wing mean aerodynamic chord, in.
S	wing area, sq ft
C_L	lift coefficient, $\frac{\text{Lift}}{qS}$
C_D	drag coefficient, $\frac{\text{Drag}}{qS}$
C_{D_0}	drag coefficient at zero lift coefficient
ΔC_{D_0}	incremental zero-lift drag coefficient (drag coefficient at any given Mach number minus drag coefficient at $M = 0.80$)
C_m	pitching-moment coefficient, $\frac{M_{\bar{c}/4}}{qS\bar{c}}$
$M_{\bar{c}/4}$	pitching moment about quarter point of \bar{c} , in-lb
$\left(\frac{dC_L}{d\alpha}\right)_{av}$	lift-curve slope, averaged over a lift-coefficient range of 0 to 0.2

$\left(\frac{dC_m}{dC_L}\right)_{av}$ static longitudinal stability parameter, averaged over a lift-coefficient range of 0 to 0.2

$(L/D)_{max}$ maximum lift-drag ratio

$\frac{dC_D}{dC_L^2}$ drag-due-to-lift factor, averaged over a lift-coefficient range of 0 to 0.3

P_b base pressure coefficient, $\frac{P_b - p}{q}$

p_b static pressure at model base, lb/sq ft

p free-stream static pressure, lb/sq ft

APPARATUS

The wing used in the present investigation was a modification of the unswept wing reported in reference 2, the outer 20 percent of each semispan having been removed leaving a wing with 0° sweepback of the quarter-chord line, an aspect ratio of 2.67, and a taper ratio of 0.2. The wing, constructed of solid 14ST aluminum alloy, had 4-percent-thick symmetrical circular-arc airfoil sections parallel to the plane of symmetry with the maximum thickness located at the 40-percent-chord station. The first combination tested, to be designated as the basic combination, had a curved fuselage. The second, or indented combination, had a body which was indented in the region of the wing-body juncture so that the axial distribution of cross-sectional area (taken normal to the airstream) for the wing-body combination was approximately the same as that of the basic fuselage alone. The third or equivalent body configuration was a body of revolution having approximately the same axial cross-sectional area distribution as the basic combination. Model details and dimensions are shown in figure 1 and body ordinates are presented in table I. Axial distributions of cross-sectional area for the various configurations are presented in figure 2. Because of an error in design, the area distribution for the equivalent body differs slightly from that of the basic combination and the distribution for the indented combination differs from that of the basic body alone by the amounts shown in figure 2. It is felt, however, that these slight area differences would not significantly affect the results or comparisons presented herein. The models were mounted on an internal strain-gage balance and were sting supported in the tunnel in the manner shown in reference 2.

Measurements and accuracy.- Lift, drag, and pitching moment were determined by means of the internal strain-gage balance. Coefficients are based on a total wing area of 0.96 square foot. Pitching-moment coefficients, based on a mean aerodynamic chord of 8.267 inches, are referred to the quarter point of the mean aerodynamic chord. Measured coefficients are estimated to be accurate within the following limits:

C_L	±0.01
C_D	±0.001
C_m	±0.003

Model angle of attack was measured by means of the fixed-pendulum, strain-gage unit described in reference 2. The unit was mounted in the model nose, and angles of attack are estimated to be accurate within $\pm 0.1^\circ$.

Static pressure at the model base was obtained from four orifices equally spaced around the sting support slightly forward of the plane of the model base (fig. 1).

Local deviations from the average free-stream Mach number did not exceed 0.003 at subsonic speeds and did not become greater than about 0.010 as Mach number was increased to 1.13 (ref. 5).

The effects of boundary-reflected disturbances in the slotted test section of the Langley 8-foot transonic tunnel on the results presented were small (refs. 5 and 6). To reduce these effects further, the model was offset vertically approximately 3.5 inches below the tunnel center line at zero angle of attack to minimize any focussing effects of the reflected disturbances, and the cross-plotted drag data have been faired at Mach numbers higher than 1.03 in an effort to eliminate the effects of the reflected disturbances.

Reynolds number for the present investigation based on the mean aerodynamic chord varied from 2.5×10^6 to 2.6×10^6 .

RESULTS AND DISCUSSION

The results presented herein have been adjusted to a condition at which the static pressure at the model base and the free-stream static pressure are equal. Base pressure coefficients for the configurations tested are presented in figure 3.

Basic data are shown as angle of attack, drag coefficient, and pitching-moment coefficient as a function of lift coefficient in

figure 4. Analysis figures, prepared from these basic data, are presented as figures 5 to 9.

Drag at constant lift coefficient.-- The variation with Mach number of drag coefficient at constant lift coefficient for the configurations tested is shown in figure 5. In addition, to provide a comparison of the severity of the transonic drag rise (based upon a Mach number of 0.80) for the various configurations, the variation of the incremental zero-lift drag coefficient ΔC_{D_0} with Mach number is also presented. The results indicate that, at Mach numbers above about 0.93 and at lift coefficients of 0 and 0.3, body indentation resulted in a substantial reduction in drag due to a reduction in adverse wing-body interference. The reduction in total drag coefficient at zero lift and a Mach number of 1.0 amounted to 31 percent. As would be expected, the beneficial effects of indentation decreased as Mach number was increased above the design condition of 1.0. The variation of the incremental zero-lift drag coefficient ΔC_{D_0} with Mach number shows that body indentation resulted in a 60-percent decrease of the transonic drag rise associated with the wing at a Mach number of 1.0. The variations of ΔC_{D_0} with Mach number for the equivalent area body and the basic configuration are approximately the same. The drag rise for the equivalent body begins earlier, however, and is slightly more severe than that of the basic configuration. The variations of ΔC_{D_0} for the indented combination and for the basic body alone indicate poor agreement for these configurations having comparable area distributions. Probable reasons for the incomplete reduction in drag for the indented combination are discussed in reference 7 for an indented delta-wing-body combination.

Shown in figure 6 is the variation with Mach number of the zero-lift drag coefficient and the incremental zero-lift drag coefficient for the basic and indented combinations of the present investigation and those of reference 2. It should be noted that in addition to removal of the pointed wing tips and the change in afterbody shape, the combinations of the present investigation differed from those of reference 2 in that there was a change in sting-support configuration. The sting support of reference 2 was cylindrical from the base of the model rearward, while that of the present investigation was expanded rearward from the model base (see ref. 2 and fig. 1). Data presented in reference 8 for a delta-wing-body combination indicate that a similar removal of the pointed tips had virtually no effect on the drag at zero lift at Mach numbers up to 0.86. At higher Mach numbers the effects of the difference in wing-area distributions for the two combinations are probably small. Because of the difficulty in evaluating sting effects and because of the considerable differences in base size and accompanying base pressure adjustments, caution should be used in comparing absolute drag values for the present configurations and those of reference 2.

The results presented in figure 6 indicate a subsonic drag level which is close to the same for all configurations. As would be expected from a consideration of the area developments for the boattail and cylindrical configurations, the transonic drag rise for the cylindrical afterbody configuration was less than that for the boattail combination. The use of body indentation with the two configurations resulted in nearly the same proportional reductions of the transonic drag rise at a Mach number of 1.0.

Drag due to lift.- Drag-due-to-lift data for the basic and indented combinations are presented in figure 7 as the variation with Mach number of the drag-due-to-lift factor $\frac{dC_D}{dC_L^2}$, which was taken as the slope of a straight line through C_D at $C_L = 0$ which best approximated a curve of C_D plotted against C_L^2 up to a lift coefficient of 0.3. It should be noted that, although the level of drag due to lift is higher for the indented combination at all but the highest test Mach number, the data of figure 4(b) show that, at Mach numbers of 0.96 and higher, the total drag for the indented combination is considerably lower than that of the basic combination up to the highest lift coefficients tested.

Maximum lift-drag ratio.- The effects of body indentation on maximum lift-drag ratio and C_L for $(L/D)_{\max}$ are shown in figure 8. Indentation resulted in an increase in the values of $(L/D)_{\max}$ at Mach numbers of 0.93 and higher, the increase at a Mach number of 1.0 amounting to 16 percent. These increased values are a result of the decrease in drag at low lift coefficients resulting from indentation. The lift coefficient for maximum lift-drag ratio $C_{L(L/D)_{\max}}$ was reduced at all but the highest test Mach number by body indentation.

Lift and pitching-moment characteristics.- The variations of average lift-curve slope $\left(\frac{dC_L}{d\alpha}\right)_{av}$ and pitching-moment curve slope $\left(\frac{dC_m}{dC_L}\right)_{av}$ for the basic and indented configurations are shown in figure 9. These data, along with the basic data presented in figures 4(a) and 4(c), indicate that body indentation had relatively little effect on the lift and longitudinal stability characteristics of the configurations tested.

CONCLUDING REMARKS

The results of the present investigation indicate that for an unswept-wing—boattail—afterbody configuration, body indentation resulted in a considerable reduction in drag at lift coefficients up to the highest tested ($C_L \approx 0.6$) at Mach numbers from 0.96 to 1.15. Maximum lift-drag ratios were increased by body indentation at Mach numbers higher than 0.93, the increase at a Mach number of 1.0 amounting to 16 percent.

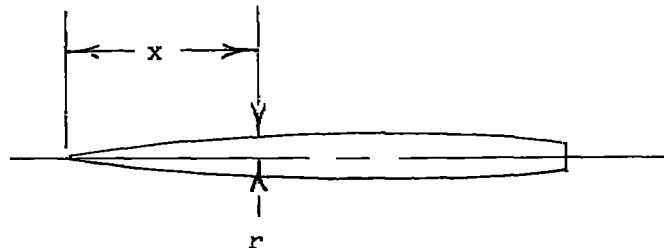
The transonic drag rise for the cylindrical afterbody configuration was less severe than that for the boattail configuration, while the use of body indentation with both configurations resulted in nearly the same proportional reductions of the transonic drag rise at a Mach number of 1.0.

Langley Aeronautical Laboratory,
National Advisory Committee for Aeronautics,
Langley Field, Va., December 23, 1953.

REFERENCES

1. Whitcomb, Richard T.: A Study of the Zero-Lift Drag-Rise Characteristics of Wing-Body Combinations Near the Speed of Sound. NACA RM L52H08, 1952.
2. Williams, Claude V.: A Transonic Wind-Tunnel Investigation of the Effects of Body Indentation, As Specified by the Transonic Drag-Rise Rule, on the Aerodynamic Characteristics and Flow Phenomena of an Unswept-Wing-Body Combination. NACA RM L52L23, 1953.
3. Robinson, Harold L.: A Transonic Wind-Tunnel Investigation of the Effects of Body Indentation, As Specified by the Transonic Drag-Rise Rule, on the Aerodynamic Characteristics and Flow Phenomena of a 45° Sweptback-Wing-Body Combination. NACA RM L52L12, 1953.
4. Estabrooks, Bruce B.: Transonic Wind-Tunnel Investigation of an Unswept Wing in Combination With a Systematic Series of Four Bodies. NACA RM L52K12a, 1953.
5. Ritchie, Virgil S., and Pearson, Albin O.: Calibration of the Slotted Test Section of the Langley 8-Foot Transonic Tunnel and Preliminary Experimental Investigation of Boundary-Reflected Disturbances. NACA RM L51K14, 1952.
6. Osborne, Robert S., and Mugler, John P., Jr.: Aerodynamic Characteristics of a 45° Sweptback Wing-Fuselage Combination and the Fuselage Alone Obtained in the Langley 8-Foot Transonic Tunnel. NACA RM L52E14, 1952.
7. Whitcomb, Richard T.: Recent Results Pertaining to the Application of the "Area Rule." NACA RM L53I15a, 1953.
8. Palmer, William E.: Effect of Reduction in Thickness From 6 to 2 Percent and Removal of the Pointed Tips on the Subsonic Static Longitudinal Stability Characteristics of a 60° Triangular Wing in Combination With a Fuselage. NACA RM L53F24, 1953.

TABLE I.- BODY ORDINATES



Forebody ordinates, all configurations	
Model station, x , in.	Body radius, r , in.
0	0
.225	.104
.338	.134
.563	.193
1.125	.325
2.250	.542
3.375	.726
4.500	.887
6.750	1.167
9.000	1.391
11.250	1.559
13.500	1.683
15.750	1.770
18.000	1.828
20.250	1.864
22.500	1.875

TABLE I.- BODY ORDINATES - Concluded

Afterbody ordinates					
Basic body		Indented body		Equivalent body	
Model station, x, in.	Body radius, r, in.	Model station, x, in.	Body radius, r, in.	Model station, x, in.	Body radius, r, in.
22.500	1.875	22.50	1.875	22.50	1.875
23.000	1.875	23.50	1.875	24.95	1.875
23.692	1.875	24.00	1.872	25.50	1.892
24.192	1.875	24.50	1.866	26.00	1.942
24.692	1.875	24.95	1.858	26.50	2.005
25.192	1.875	25.50	1.833	27.00	2.101
25.692	1.875	26.00	1.790	27.50	2.153
26.192	1.875	26.50	1.723	28.00	2.159
26.692	1.872	27.00	1.626	28.50	2.159
27.192	1.871	27.50	1.530	29.00	2.140
27.692	1.868	28.00	1.498	29.50	2.110
28.192	1.866	28.50	1.494	30.00	2.075
28.692	1.862	29.00	1.504	30.50	2.034
29.192	1.856	29.50	1.522	31.00	1.990
29.692	1.849	30.00	1.545	31.50	1.942
30.192	1.839	30.50	1.569	32.00	1.892
30.692	1.825	31.00	1.592	32.50	1.843
31.192	1.808	31.50	1.614	33.00	1.796
31.692	1.789	32.00	1.634	33.50	1.748
32.192	1.768	32.50	1.650	34.00	1.703
32.692	1.745	33.00	1.657	34.50	1.660
33.192	1.720	33.50	1.658	35.00	1.621
33.692	1.694	34.00	1.651	35.25	1.603
34.192	1.667	34.50	1.639	36.90	1.467
34.692	1.638	35.00	1.619	37.50	1.408
35.192	1.608	35.25	1.603	38.00	1.355
35.692	1.570	36.90	1.467	38.50	1.298
36.192	1.531	37.50	1.408	39.00	1.235
36.692	1.486	38.00	1.355	39.50	1.167
36.900	1.467	38.50	1.298	40.00	1.100
37.50	1.408	39.00	1.235	40.50	1.030
38.00	1.355	39.50	1.167	41.25	.937
38.50	1.298	40.00	1.100		
39.00	1.235	40.50	1.030		
39.50	1.167	41.25	.937		
40.00	1.100				
40.50	1.030				
41.25	.937				

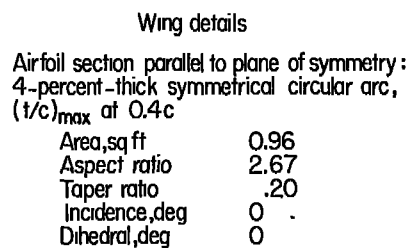


Figure 1.- Details of the wing-body combinations. All dimensions are in inches.

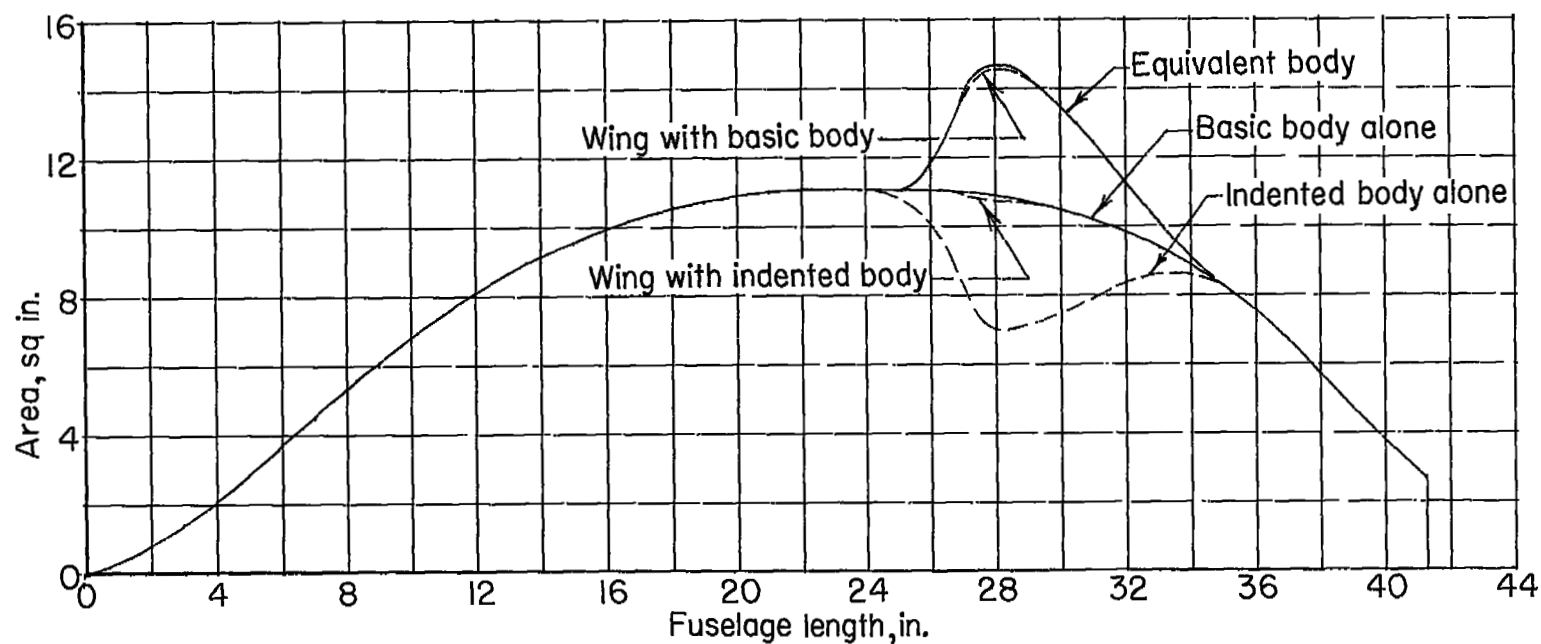
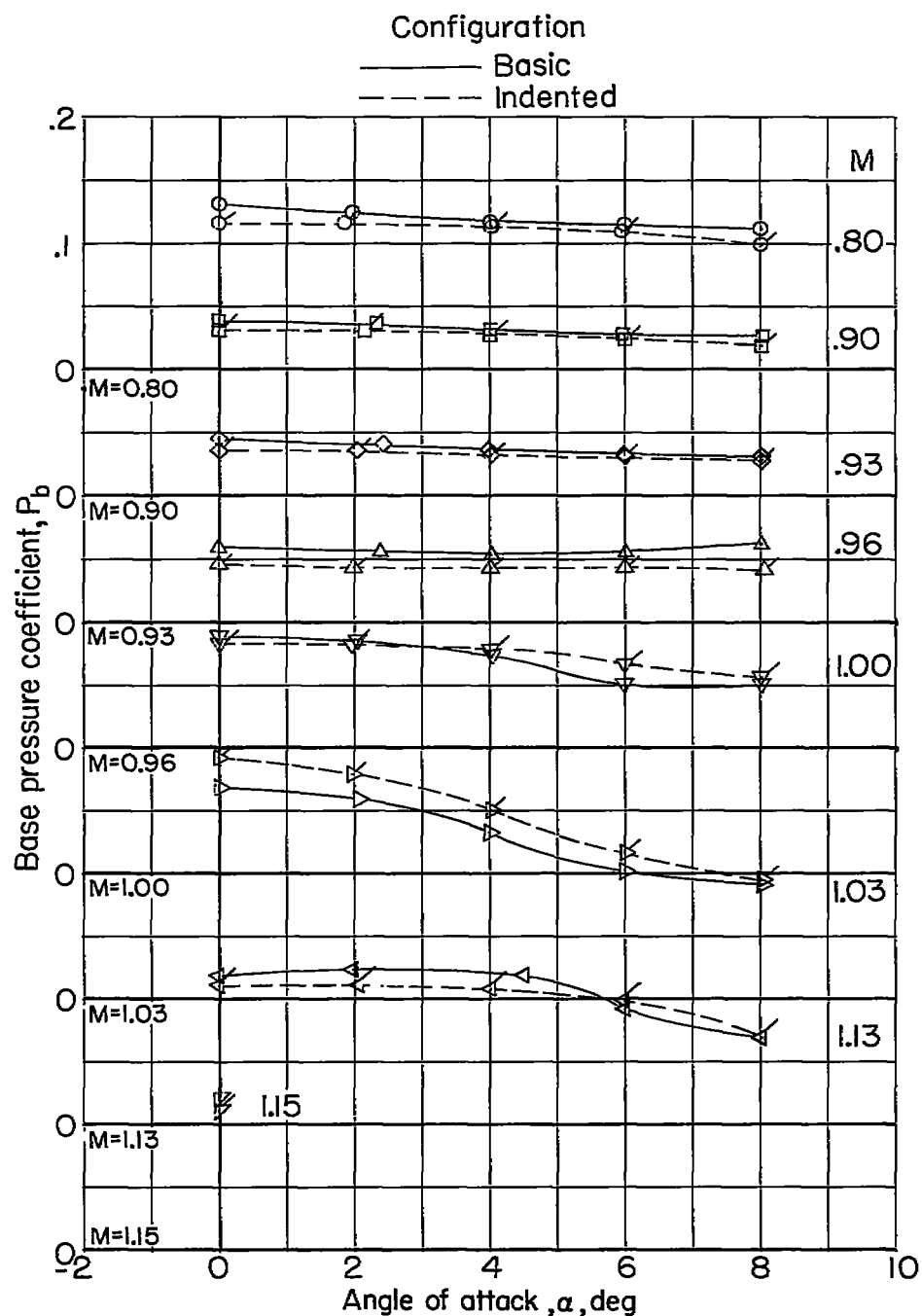
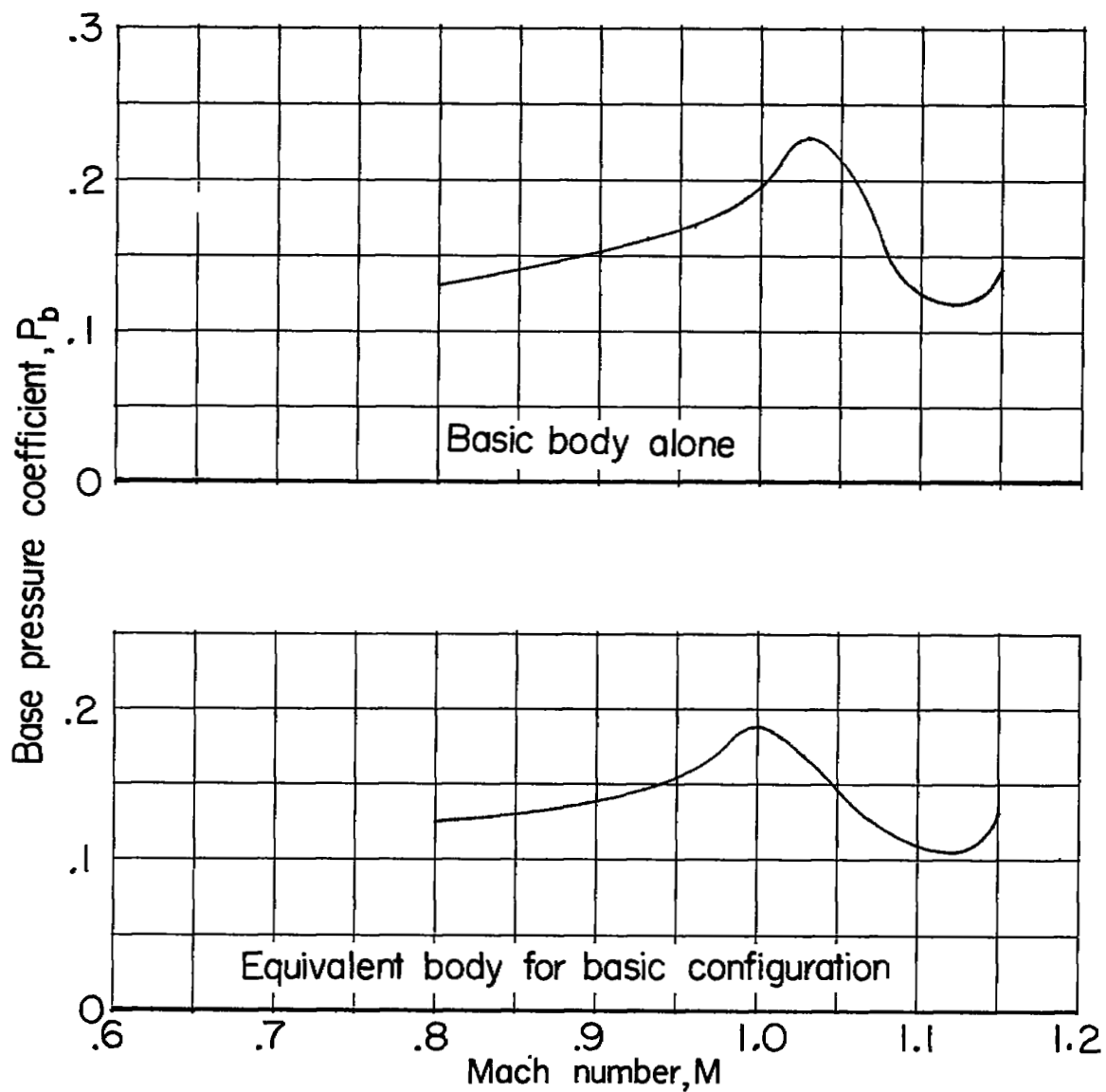


Figure 2.- Axial cross-sectional area developments for the various configurations.



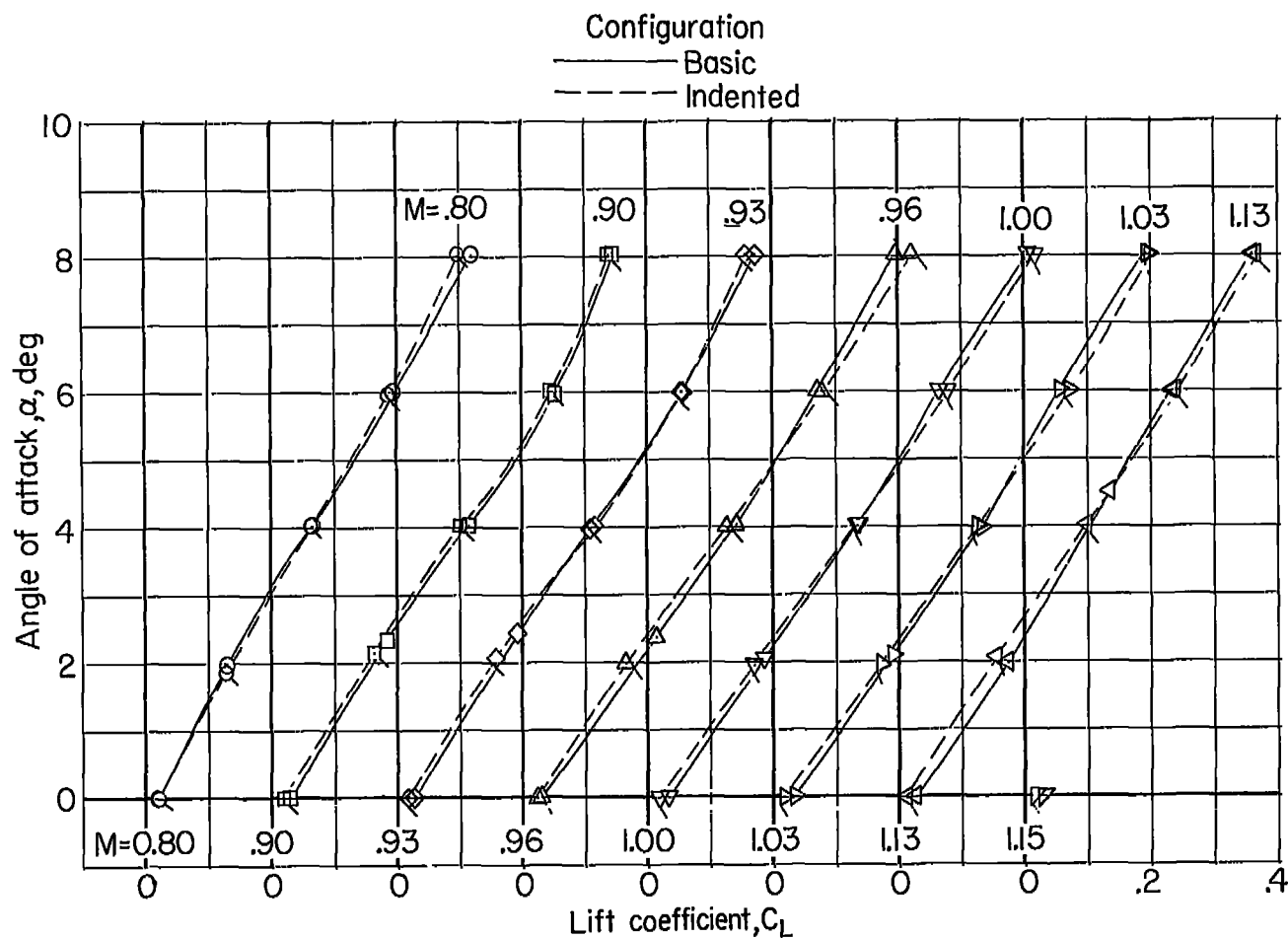
(a) Wing-body configurations.

Figure 3.- Variation of the base pressure coefficients for the various configurations.



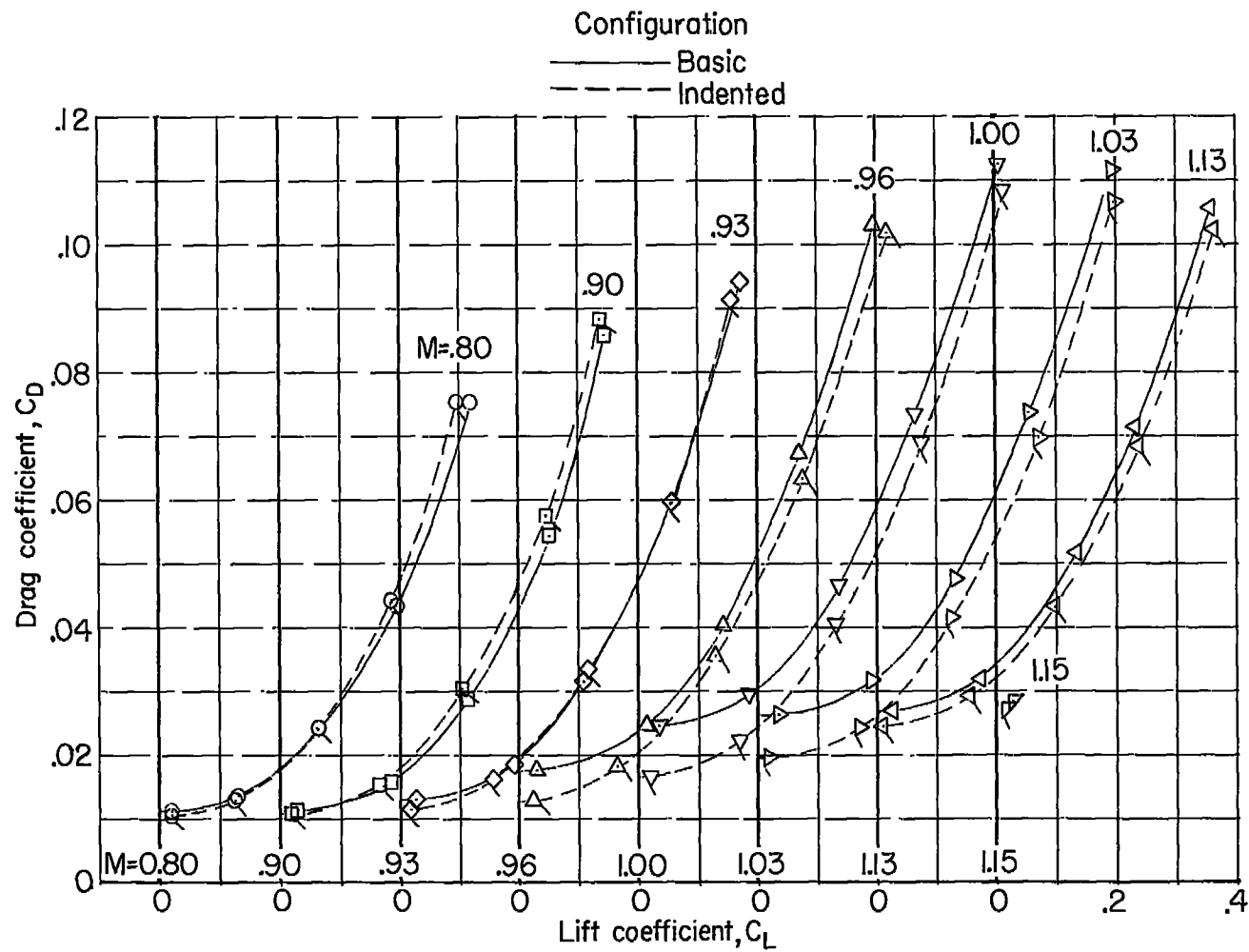
(b) Bodies alone. $\alpha = 0^\circ$.

Figure 3.- Concluded.



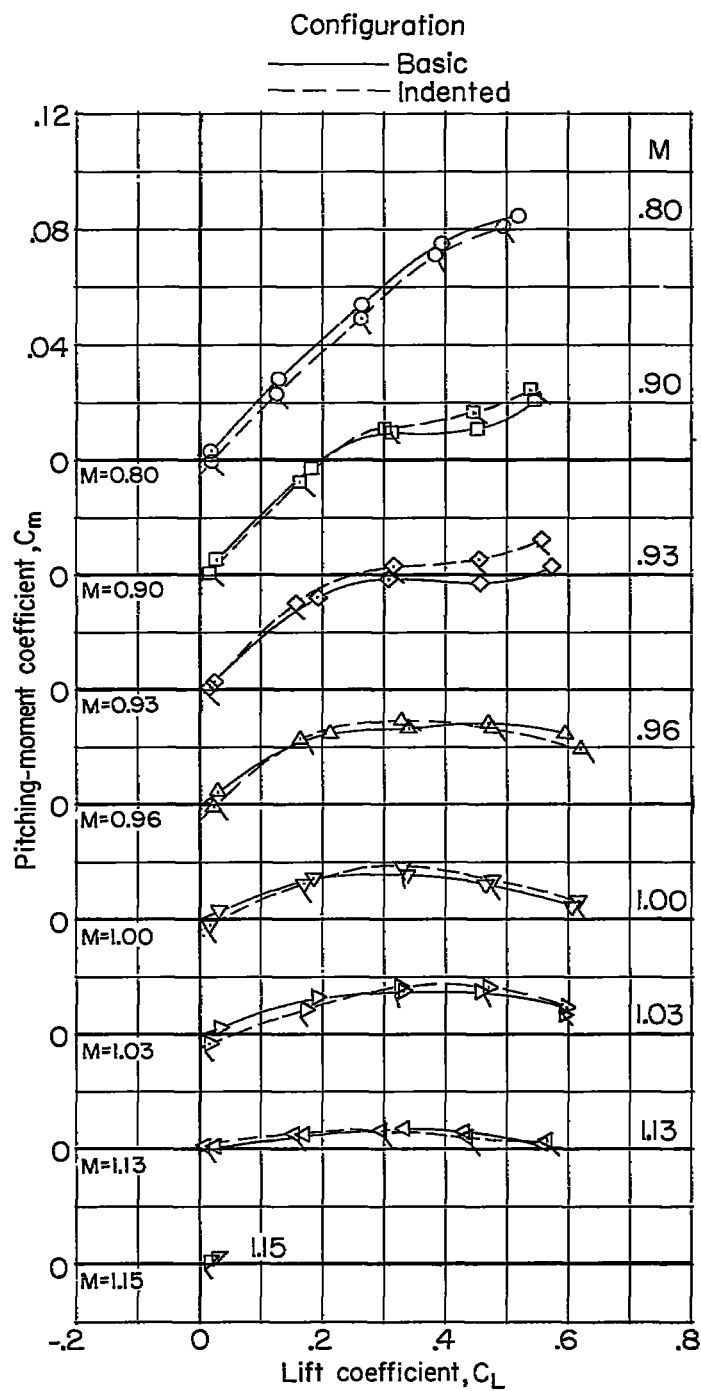
(a) Angle of attack.

Figure 4.- Variation with lift coefficient of the force and moment characteristics for the basic and indented configurations.



(b) Drag coefficient.

Figure 4.- Continued.



(c) Pitching-moment coefficient.

Figure 4.- Concluded.

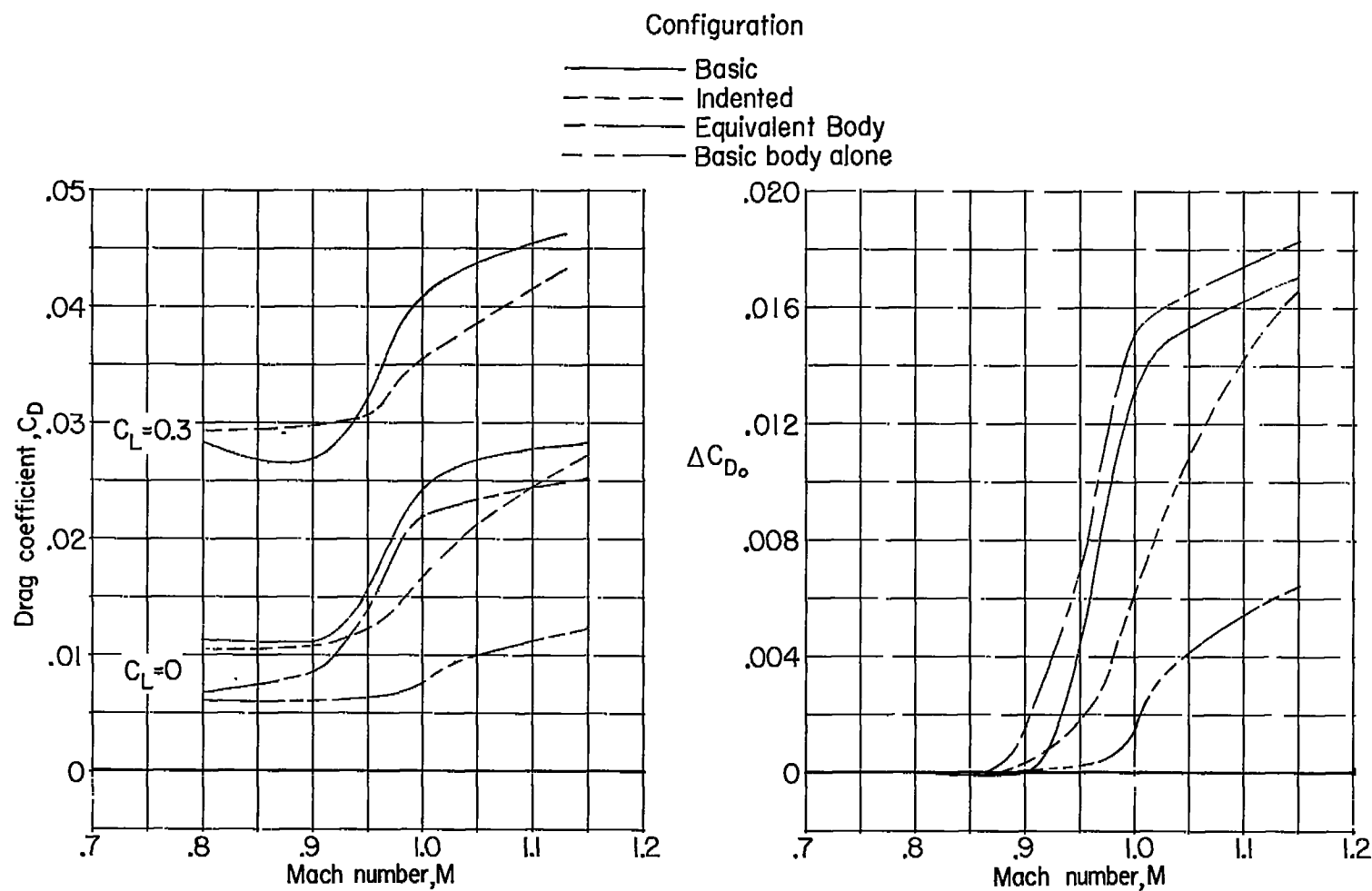


Figure 5.- Variation with Mach number of drag coefficient at constant lift coefficient and incremental zero-lift drag coefficient for the various configurations.

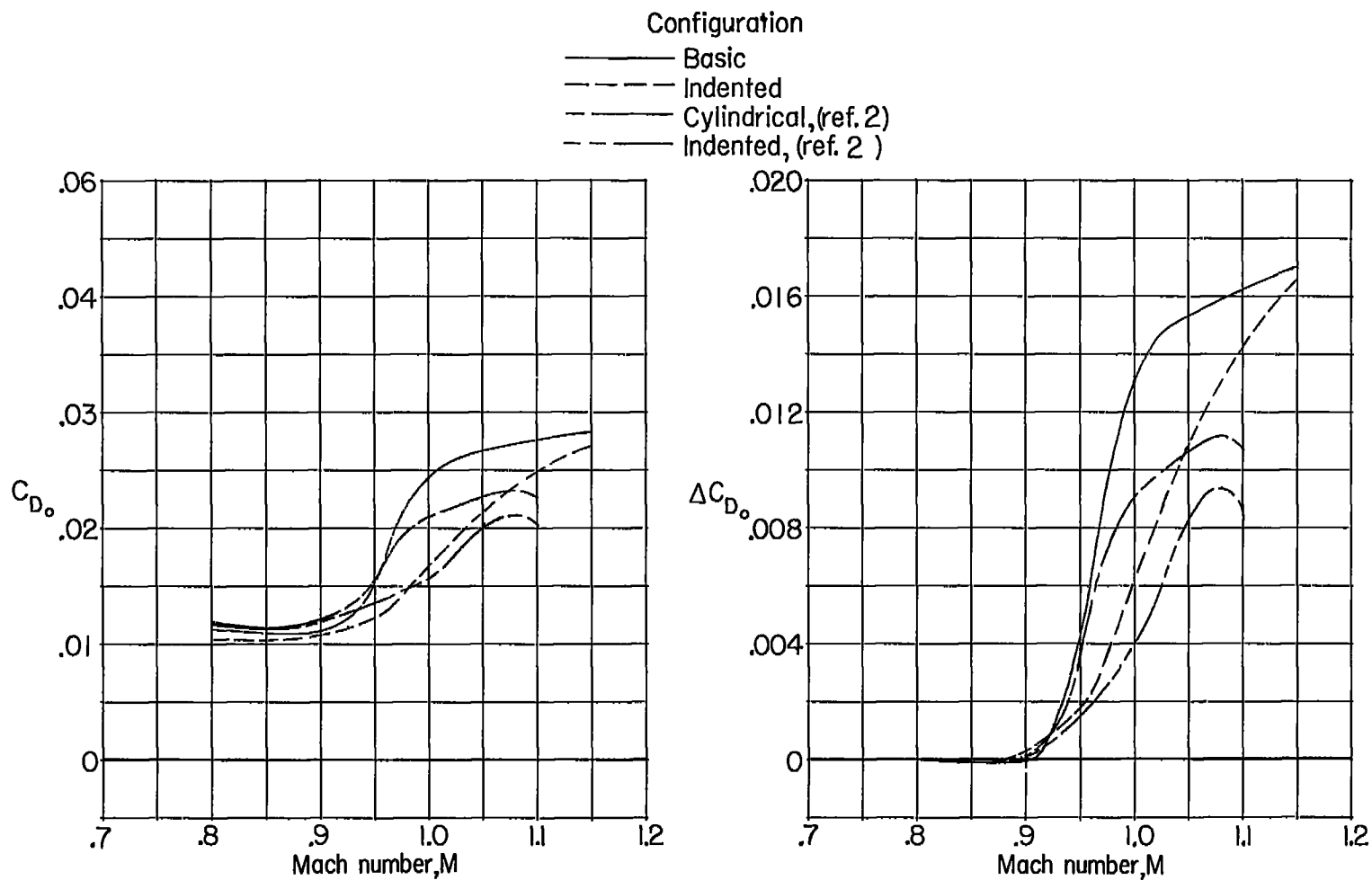


Figure 6.- Effect of afterbody shape on the variation with Mach number of drag coefficient at zero lift coefficient and incremental zero-lift drag coefficient.

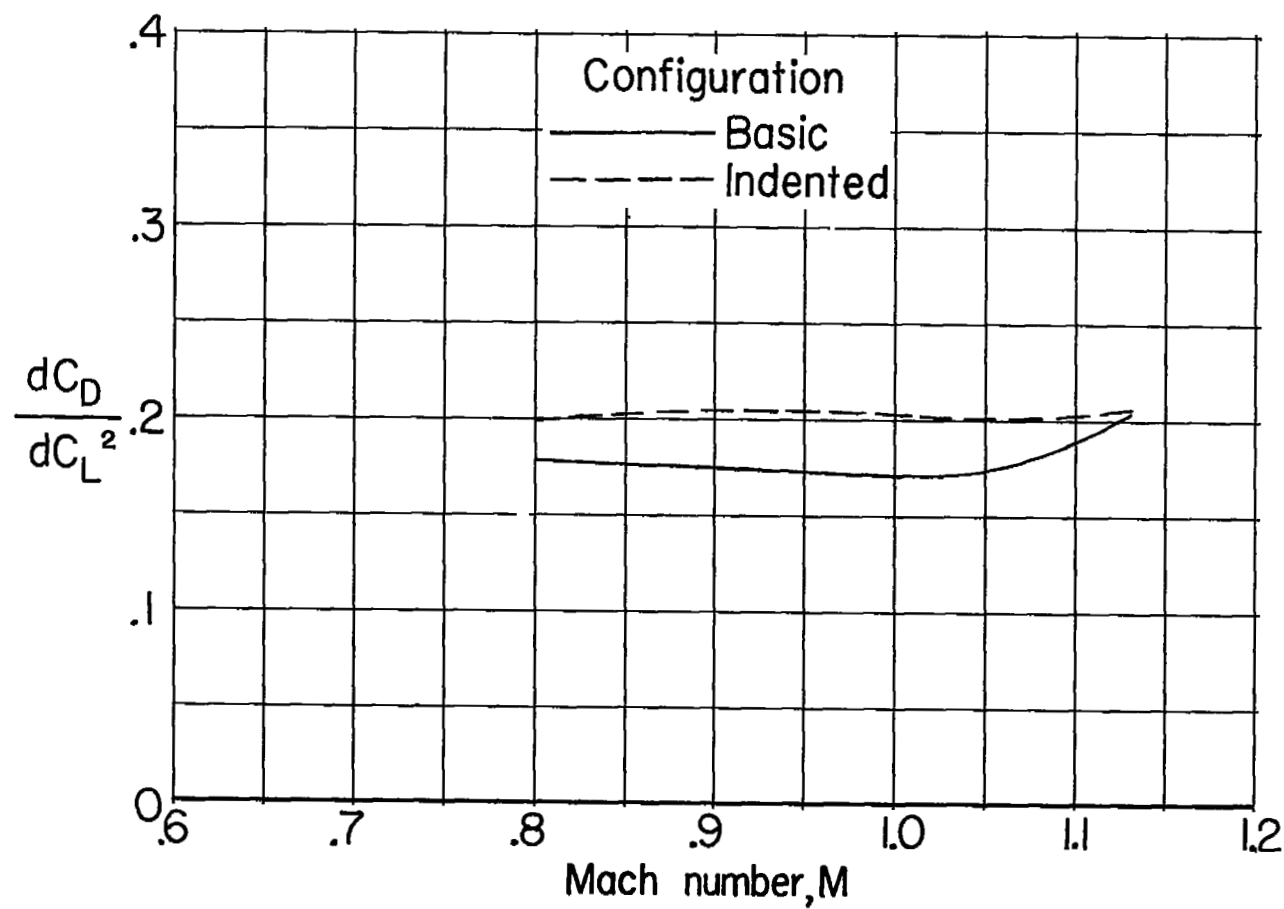


Figure 7.- Effect of body indentation on drag due to lift. $\frac{dC_D}{dC_L^2}$ averaged over a C_L range of 0 to 0.3.

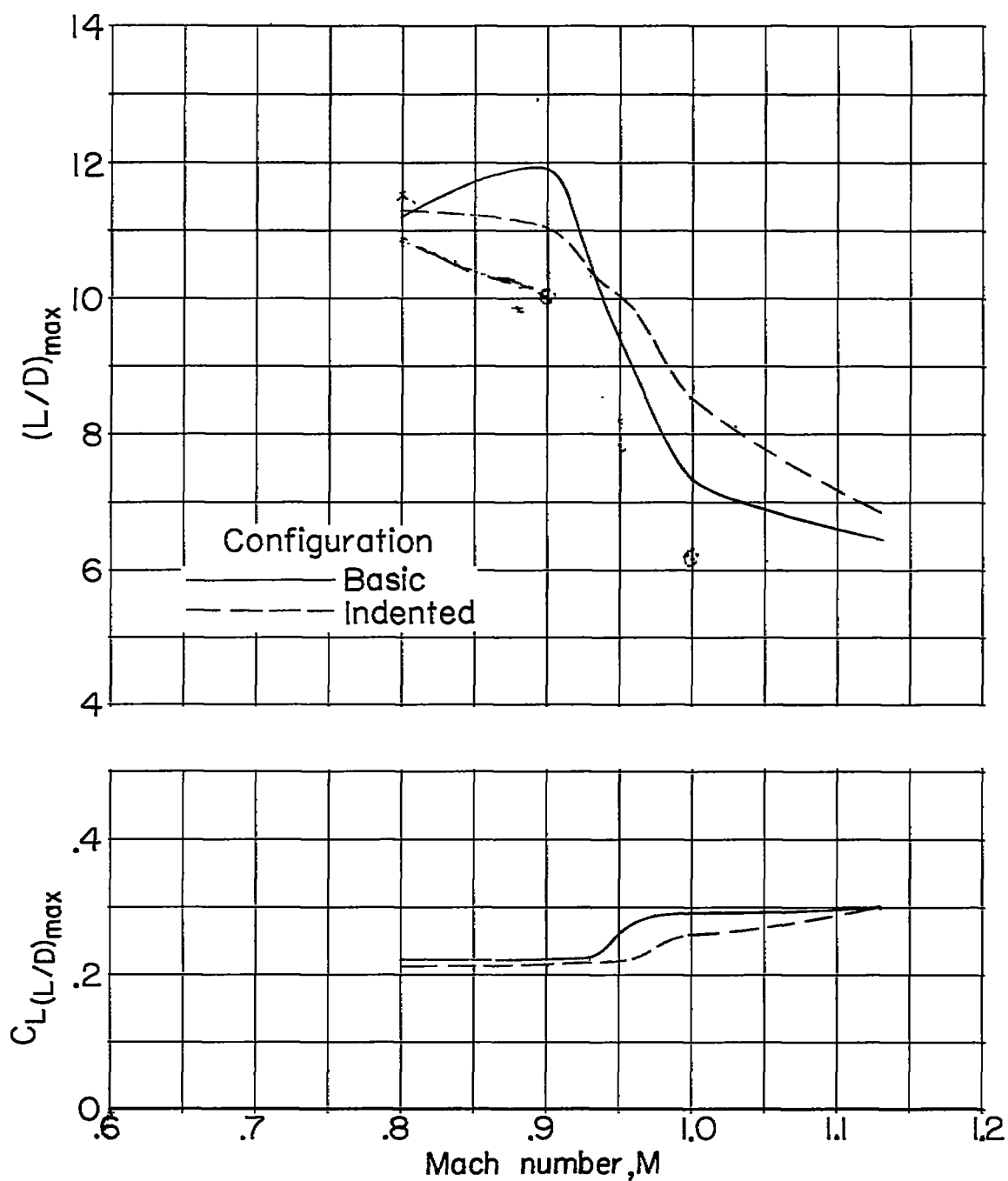


Figure 8.- Effect of body indentation on maximum lift-drag ratio and lift coefficient for maximum lift-drag ratio.

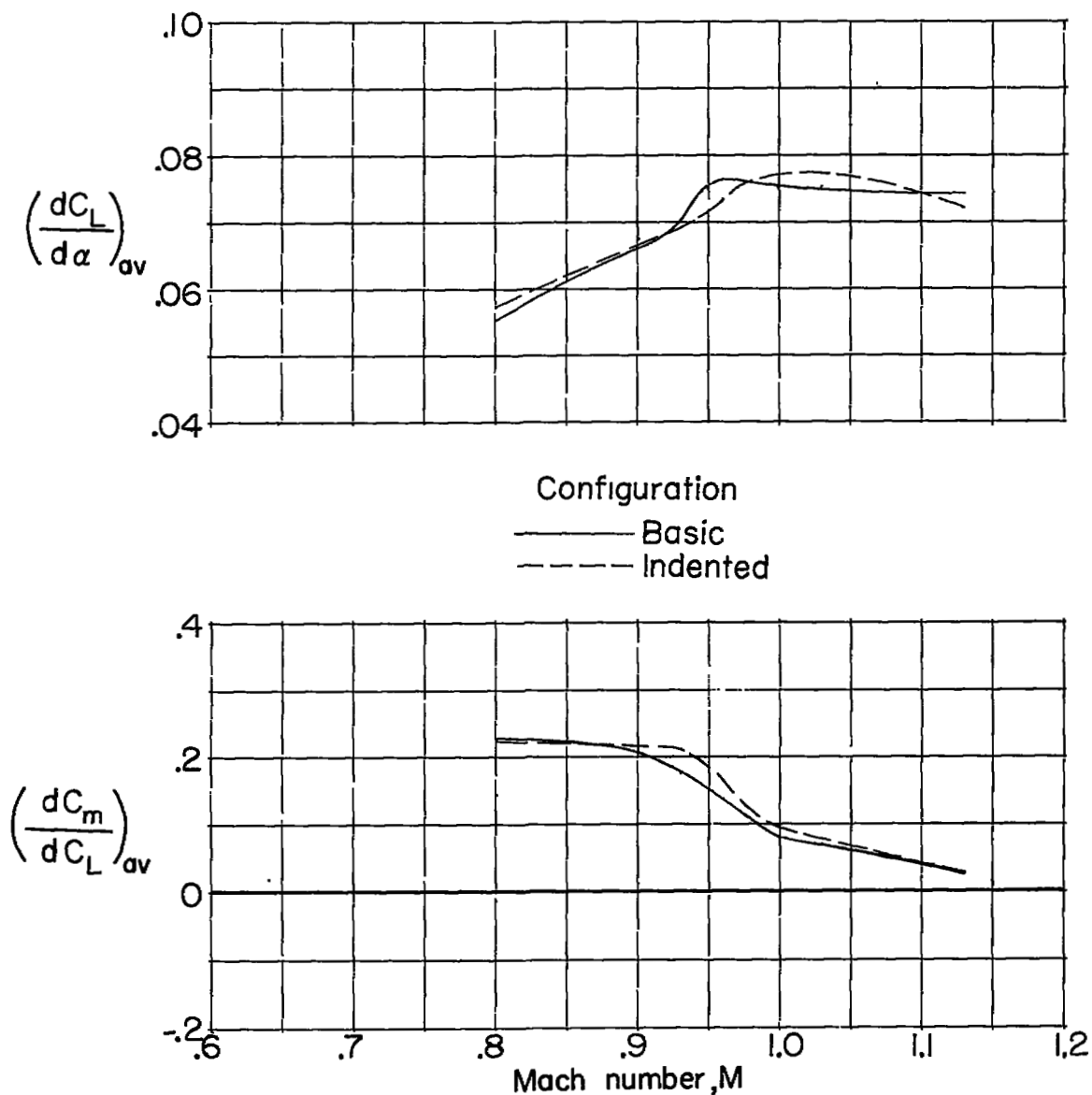
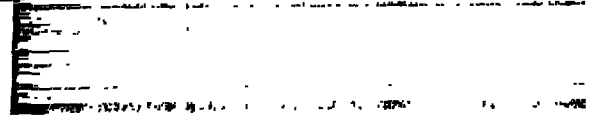


Figure 9.- Variation with Mach number of the lift-curve and pitching-moment curve slopes averaged over a C_L range of 0 to 0.2 for the basic and indented configurations.

NASA Technical Library



3 1176 01437 6165



~~CONFIDENTIAL~~